AMBIGUOUS MOMENT TENSORS AND RADIATION PATTERNS IN ANISOTROPIC MEDIA WITH APPLICATIONS TO THE MODELING OF EARTHQUAKE MECHANISMS IN W-BOHEMIA

D. RÖSSLER[1], G. RÜMPKER[2], F. KRÜGER[1]

1 Institut für Geowissenschaften, Universität Potsdam, K. Liebknecht Str. 24, 14476 Golm, FR Germany, (diroess@rz.uni-potsdam.de, kruegerf@rz.uni-potsdam.de)
2 GeoForschungsZentrum Potsdam, Telegrafenberg, 14473 Potsdam, FR Germany, (rumpker@gfz-potsdam.de)

Received: 2 June 2003; Revised: 17 October 2003, Accepted: 5 November 2003

ABSTRACT

Anisotropic material properties are usually neglected during inversions for source parameters of earthquakes. In general anisotropic media, however, moment tensors for pure-shear sources can exhibit significant non-double-couple components. Such effects may be erroneously interpreted as an indication for volumetric changes at the source. Here we investigate effects of anisotropy on seismic moment tensors and radiation patterns for pure-shear and tensile-type sources. Anisotropy can significantly influence the interpretation of the source mechanisms. For example, the orientation of the slip within the fault plane may affect the total seismic moment. Also, moment tensors due to pure-shear and tensile faulting can have similar characteristics depending on the orientation of the elastic tensor. Furthermore, the tensile nature of an earthquake can be obscured by near-source anisotropic properties. As an application, we consider effects of inhomogeneous anisotropic properties on the seismic moment tensor and the radiation patterns of a selected type of micro-earthquakes observed in W-Bohemia. The combined effects of near-source and along-path anisotropy cause characteristic amplitude distortions of the P, S1 and S2 waves. However, the modeling suggests that neither homogeneous nor inhomogeneous anisotropic properties alone can explain the observed large non-double-couple components.

The results also indicate that a correct analysis of the source mechanism, in principle, is achievable by application of anisotropic moment tensor inversion.

K e y w o r d s : anisotropy, radiation pattern, seismic moment tensor, W-Bohemia

1. INTRODUCTION

Most present studies of seismic source mechanisms are based on the assumption that the material in which the rupture occurs, as well as the medium along the ray path are isotropic. On the other hand, seismic anisotropy is a widely observed characteristic of crustal rocks and mantle material (*Babuška and Cara, 1991*). Preferred mineral

orientation due to frozen-in material flux, non-hydrostatic pressure, layering, and fracturing with preferred orientation are among the possible causes. A clear observation of crustal anisotropy has been reported for the W-Bohemian region, where observations of shear-wave splitting from the 1985/86 swarm episode were interpreted in terms of the Schoenberg-Douma fracture model (*Vavryčuk, 1993*). This model suggests transverse isotropy of about 6% for S waves with a horizontal axis of symmetry pointing N31°E.

Anisotropic material properties affect the earthquake radiation pattern and may influence the interpretation of the source mechanism. Non-double-couple components of the seismic moment tensor have been frequently observed in volcanic regions (see e.g. *Sykes, 1972*; *Solomon and Julian, 1974*; *Julian et al., 1997*; *Vavryčuk, 2002*). Such observations are often interpreted in terms of volumetric changes in the source region related to e.g. tensile faulting, explosions, or volume collapses. However, apparent volumetric source effects may also be caused by multiple shearing on non-planar faults, heterogenous focal areas, and anisotropic elastic properties (*Julian et al., 1998*). The latter is supported by the modeling of *Kawasaki and Tanimoto (1981)* who found significant non-quadrant-type radiation patterns for pure shear sources in anisotropic media. Further studies on source radiation by *Ben-Menahem et al. (1991)* and *Gajewski (1993)* endorse these findings.

For the 1997 swarm episode in W-Bohemia, moment tensor solutions for 70 earthquakes were found to be characterized by pure shear sources as well as by significant non-double-couple components (*Dahm et al., 2000*; *Horálek et al., 2000*; *Vavryčuk, 2002*). The latter were interpreted by a certain amount of tensile faulting, i.e. slip within a fault plane accompanied by crack opening or closing (*Vavryčuk, 2002*).

In the following, we will investigate possible effects of anisotropy on moment tensors and radiation patterns for earthquakes of the W-Bohemia region. Anisotropic material properties at the source can be different from those of the surrounding material (*Julian et al., 1998*; *Scholz, 1997*). We will take this into account by applying expressions for the ray-theoretical Green's function in inhomogeneous anisotropic media (*Pšenčík and Teles, 1996*). After a brief review of the theoretical background, we consider moment tensors and radiation patterns for pure-shear and tensile faulting. Effects of a rotation of the elastic tensor on the radiation are considered in some detail. Subsequently, we consider possible scenarios for anisotropic structures in the W-Bohemia region. The resulting radiation patterns are used to assess the significance of anisotropic effects on moment-tensor inversions for this region.

2. THEORETICAL BACKGROUND

The far-field displacement u_i generated by a seismic source is expressed in terms of a convolution of the spatial derivative of the Green's function $G_{ij,k}$ with the seismic moment tensor M_{jk}, which represents the equivalent forces at the source (*Aki and Richards, 2002*)

$$u_i(\mathbf{x},t) = G_{ij,k}(\mathbf{x},t,\mathbf{x}_0,t_0) * M_{jk}(\mathbf{x}_0,t) \ . \tag{1}$$

Following (*Pšenčík and Teles, 1996*), for inhomogeneous anisotropic media Eq. (1) can be given in the form

$$u_i(\mathbf{x},t) = g_i(\mathbf{x})\left[\frac{\rho(\mathbf{x}_0)c(\mathbf{x}_0)}{\rho(\mathbf{x})c(\mathbf{x})}\right]^{1/2} \frac{D\, f^{(A)}\left(t-\tau(\mathbf{x})\right)}{\left|\Omega_M(\mathbf{x})\right|^{1/2}} \exp\left[i\frac{\pi}{2}k_s - i\frac{\pi}{2}k(\mathbf{x}_0,\mathbf{x})\right] , \quad (2)$$

which is a high-frequency approximation to the solution of the wave equation. Here g_i is the polarization vector, ρ is the density, c is the phase velocity, $\mathbf{x}$ is the spatial coordinate and $f^{(A)}$ is the analytical signal corresponding to the source-time function. The index 0 denotes quantities at the source. Depending on the principle curvature of the slowness surface for a particular wavetype k_s and k can attain values of 0, 1, 2 (see *Pšenčík and Teles, 1996* for details). The force equivalents, polarizations and elastic properties at the source are given in terms of the directivity D. For a moment tensor source, D is given by (*Pšenčík and Teles, 1996*):

$$D(\mathbf{x}_0,\theta,\phi) = \frac{g_j(\mathbf{x}_0)M_{jk}\,p_k(\mathbf{x}_0)}{4\pi\rho(\mathbf{x}_0)c(\mathbf{x}_0)} \quad (3)$$

with components of the slowness vector p_k. Angles θ and ϕ specify the direction of the wavefront normal and the slowness vector, respectively. The quantity Ω_M in Eq. (2) describes the geometrical spreading. For a homogeneous anisotropic medium

$$\Omega_M = (v/c)^2\, K\, r^2 \quad (4)$$

which simplifies to $\Omega_M = (rc)^2$ in the isotropic case. Here, v is the group velocity, r is the hypocentral distance, and K is the Gaussian curvature of the slowness surface. The latter can be calculated using equations given by (e.g.) *Gajewski (1993)*, where the corresponding expression (see Eq. 2) for a homogeneous medium can also be found.

For an effective point source, the seismic moment tensor given in Eq. (3) depends on the slip s_i, the normal to the fault plane n_i, and the elastic parameters of the source medium c_{ijkl}:

$$M_{jk} = s_p n_q c_{pqjk} A_0 \ , \quad (5)$$

where the quantities s_i, n_i and c_{ijkl} are constant everywhere on the fault surface A_0. A decomposition of the moment tensor into its double-couple (DC), compensated linear vector dipole (CLVD) and isotropic (ISO) components is often used to characterize the source in terms of pure shear and volumetric changes. This can be performed using formulas given in *Jost and Herrmann (1989)* and *Vavryčuk (2002)*.

Effects of the slip direction on the total seismic moment

The total seismic moment M_T may be defined by (*Silver and Jordan, 1982*)

$$M_T = \sqrt{\Sigma_{j,k} M_{jk} M_{jk}/2} \ . \quad (6)$$

Consider, for example, a pure-shear point source within an anisotropic medium of orthorhombic (or higher) symmetry, where the axes of symmetry are parallel to the

coordinate axes. Using the crystallographic representation ($c_{ijkl} \rightarrow C_{ij}$, Voigt notation), the elastic tensor may be expressed as

$$C_{ij} = \begin{pmatrix} C_{11} & C_{12} & C_{13} & 0 & 0 & 0 \\ C_{12} & C_{22} & C_{23} & 0 & 0 & 0 \\ C_{13} & C_{23} & C_{33} & 0 & 0 & 0 \\ 0 & 0 & 0 & C_{44} & 0 & 0 \\ 0 & 0 & 0 & 0 & C_{55} & 0 \\ 0 & 0 & 0 & 0 & 0 & C_{66} \end{pmatrix} . \tag{7}$$

Further assuming slip sl_1 with $\mathbf{s} = s\,(1, 0, 0)$ and fault normal $\mathbf{n} = (0, 0, 1)$ (see Fig. 1), we obtain the moment tensor from (5) and (7)

$$\mathbf{M} = \begin{pmatrix} 0 & 0 & C_{55} \\ 0 & 0 & 0 \\ C_{55} & 0 & 0 \end{pmatrix} A_0\, s \ . \tag{8}$$

On the other hand, assuming slip sl_2 with $\mathbf{s} = s\,(0, 1, 0)$ and $\mathbf{n} = (0, 0, 1)$ (see Fig. 1), we find

$$\mathbf{M} = \begin{pmatrix} 0 & 0 & 0 \\ 0 & 0 & C_{44} \\ 0 & C_{44} & 0 \end{pmatrix} A_0\, s \ . \tag{9}$$

While these two examples represent force equivalents of pure double-couple characteristic, the resulting total seismic moments (6) differ as, in contrast to the isotropic case, $C_{44} \neq C_{55}$. Consequently, if anisotropy is not accounted for, quantities deduced from the observed total seismic moment (e.g. slip, strain, stress drop) may be biased.

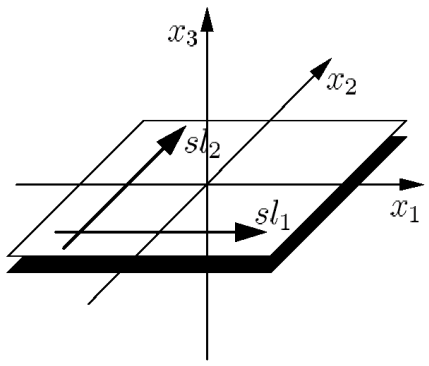

Fig. 1. Fault in the x_1-x_2-plane with slip in x_1 (slip sl_1) and x_2 direction (slip sl_2).

Table 1. Density normalized elastic constants a_{ij} taken from *Vavryčuk (1993)* for W-Bohemia (M1) and for a synthetic TI medium (M2) with 10% of anisotropy (*Rümpker and Kendall, 2002*). $[a_{ij}] = \mathrm{km}^2/\mathrm{s}^2$, $[\rho] = \mathrm{kg/m}^3$; $C_{ij} = a_{ij} \cdot \rho \cdot 10^6$.

medium	a_{11}	a_{12}	a_{13}	a_{22}	a_{23}	a_{33}	a_{44}	a_{55}	a_{66}	ρ
M1	23.5	7.8	7.8	31.9	9.9	31.9	11.0	10.8	10.8	2850
M2	39.7	13.2	13.2	39.7	13.2	32.5	10.8	10.8	13.2	2850

Taking the elastic constants derived from earthquakes in the W-Bohemia region (see Table 1, M1) as an example, the total seismic moments calculated from (8) and (9) are $30.8 \cdot 10^9$ Nm and $31.4 \cdot 10^9$ Nm, respectively (assuming unit values for s and A_0). Here, the differences can be considered negligible. However, more significant effects can be generated from different orientations of the elastic tensor or for sources in regions with stronger anisotropy.

Effects of a rotation of symmetry axes on the moment tensor

Up to this point, we have assumed that the symmetry axes of the (orthorhombic) elastic tensor are oriented parallel or perpendicular to the slip and the fault normal, respectively. Effects of a rotation of the elastic tensor with respect to the coordinate axes are elucidated by the following examples. For a general orientation of the elastic tensor in (5) with slip sl_1 the moment tensor (8) takes the form

$$\mathbf{M} = \begin{pmatrix} C_{15} & C_{56} & C_{55} \\ C_{56} & C_{25} & C_{45} \\ C_{55} & C_{45} & C_{35} \end{pmatrix} A_0 \, s \ , \tag{10}$$

where it is understood that the C_{ij} denote components of the rotated elastic tensor. In general, the trace of (10) will lead to a non-vanishing isotropic component of the moment tensor after decomposition.

We now consider a source medium given by the elastic constants derived for W-Bohemia (Table 1, M1). In a first example, we apply a rotation of $-45°$ (clockwise, the resulting medium is denoted M1$^-$) about the x_2-axis to the elastic tensor. Eq. (10) leads to

$$\mathbf{M} = \begin{pmatrix} 6.0 & 0.0 & 28.4 \\ 0.0 & 3.0 & 0.0 \\ 28.4 & 0.0 & 6.0 \end{pmatrix} A_0 \, s \cdot 10^9 \ \mathrm{Pa} \ . \tag{11}$$

Following *Vavryčuk (2002)* this tensor decomposes into components DC = 73.9%, ISO = 14.5%, and CLVD = 11.6%. Interestingly, similar values can be obtained for a tensile-type source in the original (unrotated) anisotropic medium. A unit slip, incorporating 11.5% crack opening in the x_3 direction (i.e. $\mathbf{s} = (0.993, 0, 0.115)$), would generate a seismic moment tensor with almost identical characteristics (DC = 73.8%, ISO = 14.5%, and CLVD = 11.7%).

However, the same tensile-type source can create a moment tensor with nearly vanishing non-double-couple components if the original elastic tensor is rotated by +40° (counterclockwise, M1$^+$) about the x_2-axis. In this case the decomposition leads to values that would be expected for pure shear in an isotropic medium (DC = 99.4%, ISO = 0.3%, and CLVD = 0.3%).

In conclusion, pure shear sources in generally oriented anisotropic media may lead to significant isotropic moment tensor components. The isotropic components can be of similar size as those produced by tensile-type source mechanisms. On the other hand, under certain circumstances, the tensile nature of a source may also be obscured due to anisotropy.

3. EFFECTS OF ANISOTROPY ON POINT-SOURCE RADIATION

In the following, we investigate effects of weak anisotropy on point-source radiation based on the different moment tensors discussed in the previous section. The radiation patterns are calculated from the length of the displacement vector for the particular ray direction.

Anisotropic inclusion

Anisotropy in the immediate neighborhood of the source is accounted for by the directivity function D (see Eq. 3). To investigate and isolate the effects of near-source anisotropy (i.e. an anisotropic inclusion) on the radiation pattern, we first consider isotropic material properties in the medium surrounding the inclusion. We thereby assume a smooth transition of elastic properties from the spherical anisotropic source region to the isotropic full space (i.e. along-path medium). In this model, coupling between wavetypes is considered negligible such that effects due to converted phases are not significant. It is further assumed that the ray (or group-velocity) direction is determined by the anisotropic properties of the inclusion. The isotropic properties of the along-path medium are calculated by averaging the anisotropic elastic constants (M1, Table 1) according to $v_p^2 = \left(c_{11} + c_{22} + c_{33}\right)/\left(3\rho\right)$ and $v_s^2 = \left(c_{44} + c_{55} + c_{66}\right)/\left(3\rho\right)$. Vertical cross-sections of the radiation patterns (within the x_1-x_3-plane) are given in Fig. 2. To cover the complete angular range we also show contour lines in a mercator projection (Fig. 3).

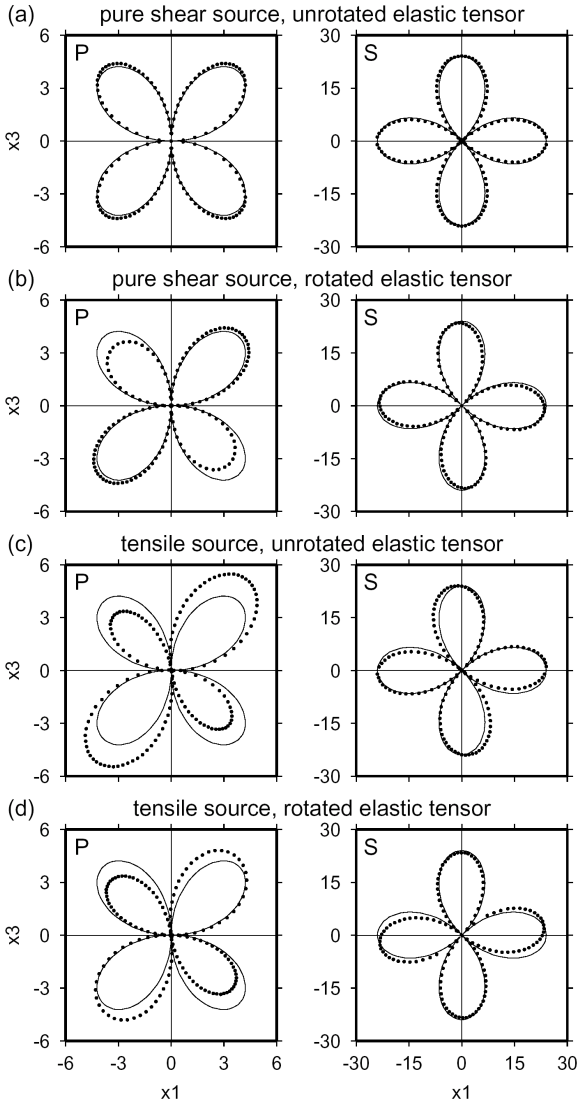

Fig. 2. Radiation patterns (dots) in the x_1-x_3-plane for P and S waves caused by four different dislocation point sources in the anisotropic inclusion (elastic constants are given in Table 1, medium M1). The surrounding (along-path) medium is assumed isotropic. (a) A pure-shear source within the anisotropic inclusion with elastic proper- ties given by medium M1. (b) The elastic tensor within the inclusion (medium $M1^-$) is rotated by $-45°$ (clockwise) about the x_2-axis. (c) The shear source is accompanied by 11.5% crack opening in the anisotropic inclusion (tensile faulting). The elastic tensor is given by medium M1. (d) The same tensile source as in (c). The elastic tensor within the inclusion is rotated by 40° (counterclockwise) about the x_2-axis (medium $M1^+$). For comparison radiation patterns for a pure-shear source in a homogeneous isotropic medium are shown (solid line). Units are given in μm.

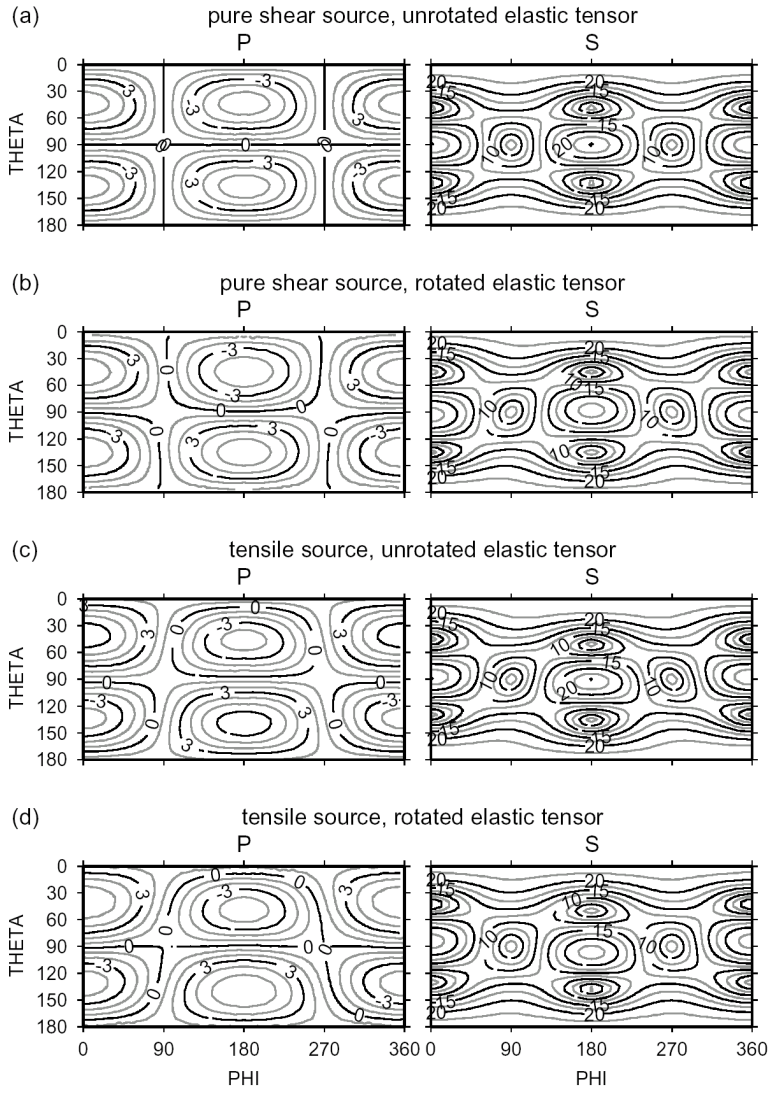

Fig. 3. Mercator projection of the P and S-wave radiation patterns for sources given in Fig. 2. Positive signs in P correspond to compressional first motion. Note that the projection leads to strong distortions in the vicinity of $\theta = 0°$ and 180°. Units of contour lines are given in μm.

i) The pure shear source (slip sl_1 in Fig. 1) in the (unrotated) anisotropic medium (M1, Figs. 2a, 3a) produces symmetric radiation patterns with crossing nodal lines (quadrant-type characteristic) for the P wave and nodal points for the S wave. The radiation patterns are similar to those found for isotropic media (see *Aki and Richards, 2002*). Note, that in this case the symmetry axis of the medium M1 is parallel to the slip direction.
ii) The same pure shear source in the rotated anisotropic medium ($M1^-$) generates considerable apparent isotropic components (Figs. 2b, 3b). Amplitudes in the directions of compression are similar to those in the previous case, whereas the amplitudes in dilatational directions are decreased. The nodal lines do not intersect which is typical for tensile sources (non-quadrant-type characteristic). However, this is in contrast to the pure-shear nature of the event. S-wave amplitudes are slightly distorted but still very similar to those in the unrotated medium.
iii) The tensile source (i.e. $\mathbf{s} = (0.993, 0, 0.115)$) in the unrotated medium (M1) produces the strongest modifications in the radiation patterns (Figs. 2c, 3c). P-wave amplitudes in the directions of compression are significantly enlarged, whereas they are decreased in the directions of dilatation. As in the previous case, nodal lines of the P-wave amplitudes do not intersect. In comparison (see ii), the amplitudes of the S waves are slightly more distorted.
iv) For most angular ranges, the P and S amplitudes of the same tensile source in the rotated medium ($M1^+$, Figs. 2d, 3d) are deformed in a way similar to the previous case. However, nodal lines of the P-wave amplitudes that nearly close up are an important feature of this source. Thus, this radiation pattern is more similar to that for the shear source in the unrotated medium (see i).

Generally, the findings agree with the previous results from the decomposition of the moment tensors for the different source mechanisms. The P-wave radiation patterns are usually more distorted. A possible explanation for this could be that (as in the isotropic case) compression and dilatation away from the source are transmitted by P rather than S waves.

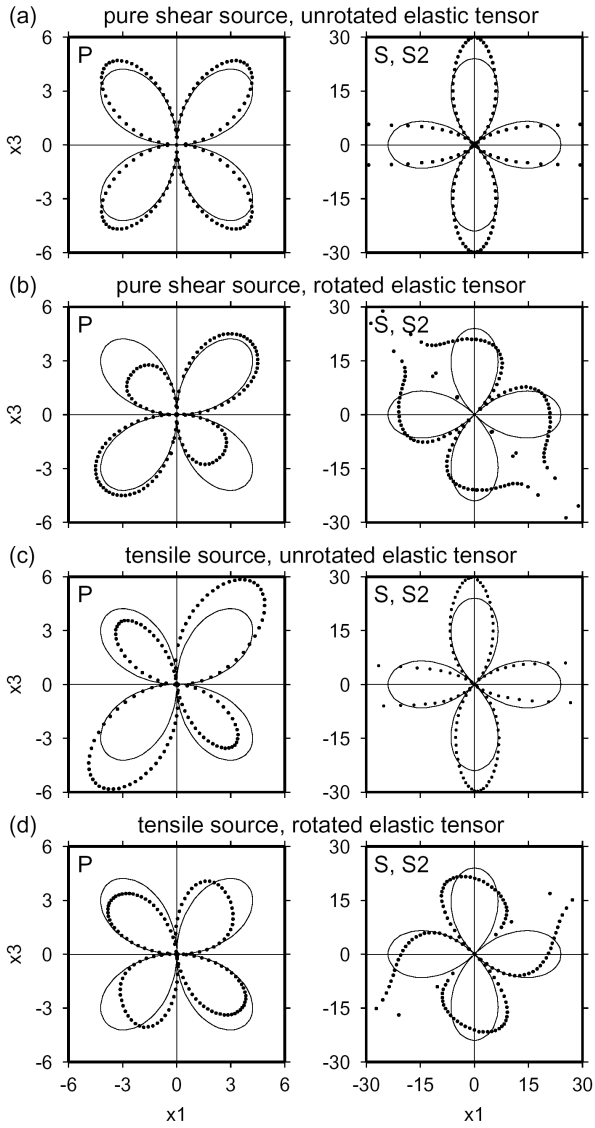

Fig. 4. Radiation patterns for the case of homogeneous anisotropy (the same anisotropic properties are used for the inclusion and the along-path medium). Otherwise as in Fig. 2.

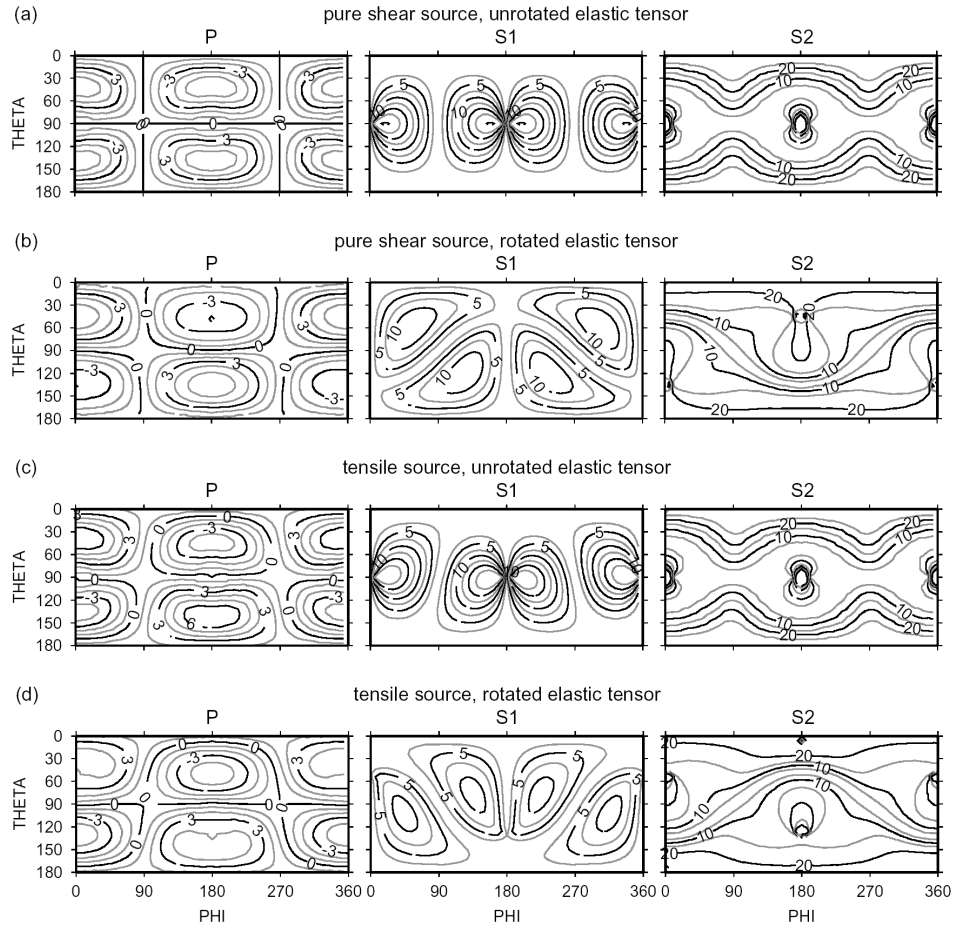

Fig. 5. Radiation patterns for the case of homogeneous anisotropy. Otherwise as in Fig. 3. The S-wave amplitudes for values of $\phi = 0°$ (360°), 180° have to be considered with care, as they may correspond to directions of slowness-surface singularities.

Homogeneous anisotropic medium

In this section the isotropic elastic tensor in the full-space is replaced by the anisotropic tensor at the source (inclusion) such that the medium becomes homogeneous. Due to the anisotropy in the medium along the ray path we now consider radiation patterns for three wavetypes P, S1, S2 (see Figs. 4 and 5 for the corresponding cross sections and contour plots).

In general, the P-wave radiation patterns in the homogeneous anisotropic case are similar to those in the previous section. The amplitude variations are slightly more pronounced. For all cases in the x_1-x_3-plane only one type of S wave (S2) is excited. The slip lies in this plane, which also corresponds to a symmetry plane of the elastic tensor. Thus, the slow S2 wave exhibits SV polarization.

For certain directions, which are related to shear-wave slowness-surface singularities in the vicinity of the x_1-axis, the high-frequency approximation for the computation of the anisotropic Green's function breaks down, leading to unphysically large values for the radiation amplitudes. For these directions the shear waves do not propagate independently leading to frequency dependent amplitude effects. The application of more complete solutions for the displacements based on integral representations is necessary to describe the corresponding waveform. These complications are not considered in the present paper.

Contours of the radiation patterns (Fig. 5) may be characterized as follows.

i) For the shear source in the unrotated medium (M1) we find quadrant-type P-wave radiation; the corresponding radiation patterns for S1 and S2 are symmetric with respect to $\theta = 90°$, which corresponds to the x_1-x_2-plane.
ii) For the shear-source in rotated medium ($M1^-$) the P-wave radiation is of non-quadrant type; the previous symmetry for the S1 and S2 radiation is lost.
iii) For the tensile source in the unrotated medium the P-wave radiation is of non-quadrant type; the S1 and S2 radiation patterns are similar to case i).
iv) For the tensile source in the rotated medium ($M1^+$), quadrant-type P radiation dominates (even more clearly as in the previous section), which could be considered a characteristic of pure shear sources. The S1 and S2 radiation patterns are distorted in a characteristic fashion.

For P waves the discrimination between quadrant and non-quadrant type radiation is obvious. For the S waves the interpretation is less clear due to the occurrence of two wavetypes. A more conclusive interpretation of the results should be based on waveform calculations and their inversion. This will be studied in more detail in a forthcoming paper.

4. CASE STUDY: MODELING OF ANISOTROPIC EFFECTS IN THE W-BOHEMIAN EARTHQUAKE REGION

The earthquakes of the W-Bohemian swarm episode of 1997 show two spatially distinct event clusters with different focal mechanisms of either small (type A) or up to about 50% (type B) non-double-couple components (see *Vavryčuk, 2002*; *Dahm et al., 2000*; *Horálek et al., 2000*). The latter have been interpreted as tensile earthquakes due to hydrofracturing (*Vavryčuk, 2002*). However, since anisotropy is also present in this region (*Vavryčuk, 1993*), we are interested in the possible consequences for the interpretation of the source mechanism. The effects of anisotropy on isotropic moment-tensor-inversion schemes have recently been investigated by *Šílený and Vavryčuk (2002)* in great detail. Here, we use a more exemplary approach, which is limited to the forward problem, but also accounts for the previously omitted effects of anisotropy on the moment tensor itself. We further consider effects of inhomogeneous anisotropic properties due to distinct near-source anisotropy (an inclusion). As before, we assume a smooth change of the elastic

properties from the source to the medium along the ray path such that effects due to wavetype conversion can be neglected. We assume that the ray direction is determined by the anisotropic properties of the along-path medium.

In the following, we present radiation patterns for pure shear sources based on the source geometry defined by events of type B. The computation of radiation patterns is carried out using Eq. (2). In our modeling, coordinates are chosen such that the x_1-axis points to the east, the x_2-axis points north, and the x_3-axis is taken positive upwards. The elastic properties of the medium along the ray-path are defined by the Schoenberg-Douma's model for the W-Bohemian swarm earthquake region of *Vavrčuk (1993)*. Here, the elastic tensor (M1, see Table 1) is rotated by 59° (counterclockwise) about the x_3-axis such that the horizontal symmetry axis points N31°E in agreement with the findings of *Vavryčuk (1993)*.

We further adopt a fault geometry similar to that for events of type B by choosing strike = 45°, dip = 90°, and rake = 45°. This corresponds to a slip vector $\mathbf{s} = (1/2, 1/2, 1/\sqrt{2})$ and a fault normal $\mathbf{n} = (1/\sqrt{2}, -1/\sqrt{2}, 0)$. We consider four cases:

Case A0: In this reference case the along-path medium is characterized by average isotropic elastic properties, whereas the anisotropic inclusion exhibits the elastic properties of medium M1. This includes a rotation about the vertical axis such that the horizontal symmetry axis aligns parallel to N31°E.

Case A1: For this homogeneous anisotropic model the entire medium exhibits the same elastic properties as the anisotropic inclusion of case A0.

Case A2 (inhomogeneous anisotropic model I): Here we assume that the fracture zone (modeled by the inclusion) exhibits strong P and S-wave anisotropy of 10% (*Crampin, 1994*) due to extreme deformation and remineralization. Further assuming mineralization in layers parallel to the fault plane, we take a generic transversely isotropic (TI) elastic tensor (M2, see Table 1) with symmetry axis parallel to the fault normal. Here, the symmetry axis corresponds to the slow direction for both P and S waves. In the surrounding medium, along the ray path, we assume the same anisotropic elastic properties as in the previous case (A1). Thus, the symmetry axis at the source lies oblique to that in the along-path medium.

Case A3 (inhomogeneous anisotropic model II): Recent studies indicate that the foci of the swarm events in W-Bohemia are located in a N-S striking shear zone (*Bankwitz et al., 2002*; *Bankwitz and Schneider, 2000*). Considering the same orienting mechanisms as in the previous case (A2), the properties of the inclusion may be characterized by TI anisotropy with an E-W oriented symmetry axis. Outside of the inclusion we assume equal anisotropic elastic properties as in the previous cases (A1 and A2).

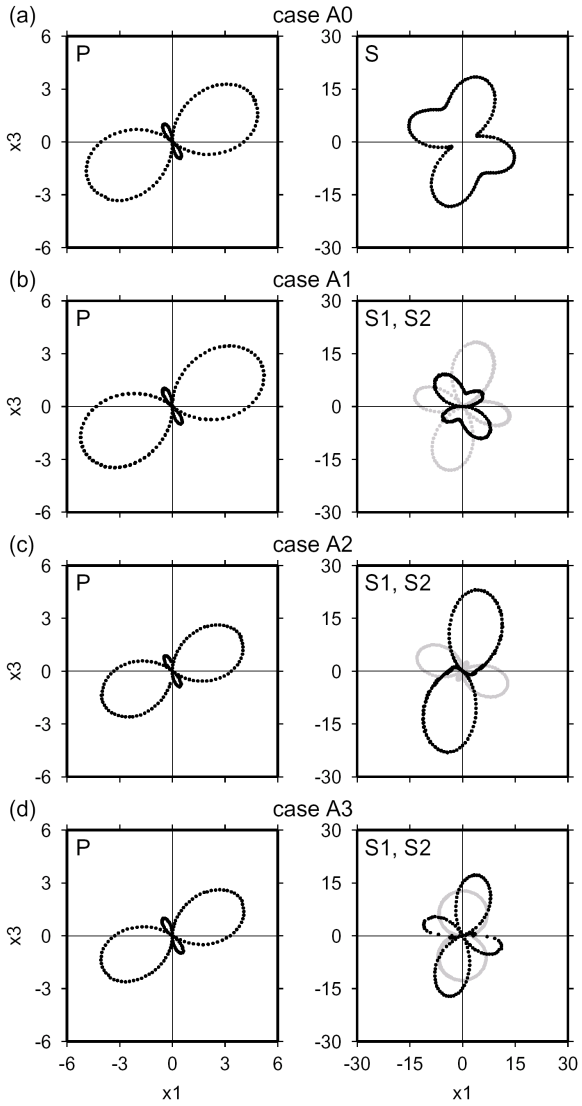

Fig. 6. Radiation patterns of the P, S1 (grey), and S2 (black) waves for faulting of type B. Here, x_1 points to the east, x_3 points upwards, oblique to the fault normal and the slip. Case A0 corresponds to the anisotropic inclusion with elastic properties given by medium M1. The surrounding along-path medium is assumed isotropic. Case A1 corresponds to homogeneous anisotropy with properties given by medium M1. Case A2 corresponds to a transversely isotropic inclusion with properties given by medium M2; the axis of symmetry is aligned with the fault normal. Case A3 corresponds to a transversely isotropic inclusion given by medium M2; the axis of symmetry points east. The surrounding medium for cases A1-A3 is given by the same elastic tensor (medium M1, see text for details). Apparent gaps in the radiation patterns are due to the irregular sampling interval in this non-symmetry plane. Units are given in μm.

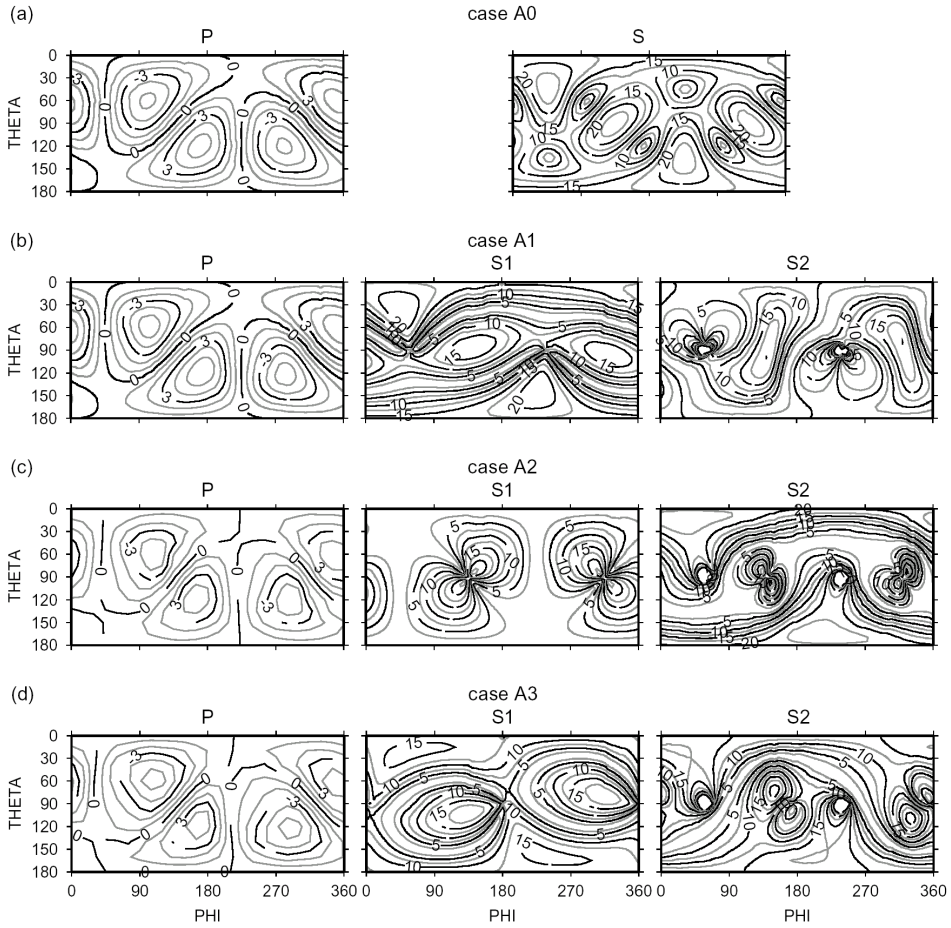

Fig. 7. Mercator projection of radiation patterns. Otherwise as in Fig. 6. Note singular directions for S waves near $\theta = 90°$ in (b)-(d).

Radiation patterns for the different cases are given in Figs. 6 and 7, respectively. The cross-sections shown in Fig. 6 correspond to the vertical E-Z plane. Note that, unlike the previous section, the fault plane is oblique to the E-Z plane such that the typical four-lobe pattern is not apparent in this representation. The findings can be summarized as follows:

i) The source for cases A0 and A1 leads to a seismic moment tensor which is dominated by double-couple components (DC = 94.1%). However, due to the oblique orientation of the fault with respect to the anisotropic symmetry planes, volumetric components (ISO = 5.1%) are created (see Table 2 for the moment tensor decomposition). The volumetric effects are relatively small; they are most apparent for P waves in

Figures 7a – b, where the nodal lines are separated. The amplitude values in dilatational and compressional regions are almost the same. While the anisotropic properties of the along-path medium have little effect on the P-wave radiation (A1), they do cause S-wave splitting which is expected to significantly affect waveforms. However, from the cross-sections it becomes apparent that summing-up the contributions from the two S waves (case A1) will lead to similar S-wave radiation patterns as in the previous case (A0).

ii) For case A2, the isotropic component of the moment tensor vanishes (see Table 2). This is because the anisotropy (TI) in the inclusion exhibits a symmetry axis parallel to the fault normal (see section 2). Contours of the P-wave radiation show closely-spaced nodal lines and nearly equal amplitudes for regions of compression and dilatation (Fig. 7c). Radiation patterns for the two S waves exhibit relatively strong differences compared to case A1.

iii) For case A3, the oblique orientation between source anisotropy and fault plane causes significant (negative) non-double-couple components of the moment tensor (DC = 77.9%, ISO = –6.5%, CLVD = –15.6%; see Table 2). The P-wave radiation pattern is intermediate between cases A1 and A2. The nodal lines are not as close as in the previous inhomogeneous case, but slightly less separated than in the homogenous case. Again, the direct interpretation of the S-wave pattern is difficult. However, comparison with the previous cases (A1, A2) suggests, that they are most sensitive to changes in anisotropic properties of the inclusion.

Table 2. Moment tensor decomposition for synthetic faulting of fault type B.

case	DC (%)	ISO (%)	CLVD (%)
A0, A1	94.1	5.1	–0.8
A2	100.0	0.0	0.0
A3	77.9	–6.5	–15.6

5. CONCLUSIONS

1) For pure-shear sources in anisotropic media the total seismic moment is sensitive to the slip direction. The decomposition of the moment tensor can lead to significantly different non-double-couple components depending on the orientation of the fault with respect to the anisotropic symmetry planes.
2) In cases where anisotropic material properties are limited to the immediate source region (i.e. an anisotropic inclusion), effects on the radiation patterns are most pronounced for P waves. The examples show that the occurrence of apparent volumetric components for pure-shear sources is determined by the orientation of the anisotropic tensor with respect to the fault and the slip. Effects of true tensile faulting may be hidden for certain orientations of the near-source anisotropy with respect to the fault.
3) Anisotropic properties in the along-path medium cause pronounced distortions of the S-wave radiation due to effects related to slowness-surface curvature and S-wave

splitting. However, to better assess the possible consequences for the interpretation of source mechanisms, the calculation of complete waveforms is required. The P-wave radiation in the homogeneous anisotropic medium is similar to the case, where anisotropy is limited to the inclusion. This indicates that little information can be gained from P-wave radiation on the extent of the anisotropic region.

4) The inhomogeneous anisotropic models for the W-Bohemia region cause significantly different radiation patterns for S waves. The P-wave amplitudes are relatively uniform. Their interpretation under isotropic assumptions would yield seismic moment tensors with dominating double-couple components and could, therefore, reveal the correct source mechanism. However, it seems possible that a moment tensor inversion for anisotropic media under inclusion of S waves can significantly improve the interpretation with respect to source anisotropy and source mechanism. Such algorithm is currently under development and will be based on waveform calculations for anisotropic media.
5) In our modeling of anisotropy in W-Bohemia, the moment tensor decomposition yields non-double-couple components of up to 22%, which includes isotropic (i.e. volumetric) components of up to 6%. These estimates cannot explain the observed large non-double-couple components. However, the moment tensor decomposition does not account for the possibly significant effects due to anisotropy of the along-path medium. Shear wave splitting and related frequency-dependent amplitude effects will affect P/S-amplitude ratios, which are indicative of volumetric effects in isotropic media. To estimate the significance of apparent tensile contributions more precisely, it would be necessary to apply a conventional isotropic inversion algorithm to synthetic waveforms for the models presented here (see *Šílený and Vavryčuk, 2002*).

Acknowledgments: We would like to thank I. Pšenčík, T. Dahm and the two anonymous referees for very helpful comments and suggestions. This work was supported by the Deutsche Forschungsgemeinschaft, grant KR 1935.

References

Aki K. and Richards P., 2002. *Quantitative Seismology.* University Science Books.

Babuška V. and Cara M., 1991. *Seismic Anisotropy In The Earth.* Kluwer Academic Publishers.

Bankwitz P., Kämpf H., Störr M. and Schneider G., 2002. Shear faults in tertiary clay formation of the Eger Basin (Czech Republic) and their role for the degassing of the uppermost mantle. *Mitt. naturwiss. Ver. Steiermark*, **132**, 31–34.

Bankwitz P. and Schneider G., 2000. Seismic and aseismic movements in the western Bohemia/Vogtland area. *Stud. Geophys. Geod.*, **44**, 611–613.

Ben-Menahem A., Gibson Jr. R. and Sena A., 1991. Green's tensor and radiation pattern of point sources in general anisotropic inhomogeneous elastic media. *Geophys. J. Int.*, **107**, 297–308.

Crampin S., 1994. The fracture criticality of crustal rocks. *Geophys. J. Int.*, **118**, 428–438.

Dahm T., Horálek J. and Šílený J., 2000. Comparison of absolute and relative moment tensor solutions for the January 1997 West Bohemia earthquake swarm. *Stud. Geophys. Geod.*, **44**, 233–250.

Gajewski D., 1993. Radiation from a point source in general anisotropic media. *Geophys. J. Int.*, **113**, 299–317.

Horálek J., Šílený J., Fischer T., Slancová A. and Boušková A., 2000. Scenario of the January 1997 West Bohemia earthquake swarm, *Stud. Geophys. Geod.*, **44**, 491–521.

Jost M. and Herrmann R., 1989. A student's guide to and review of moment tensors. *Seism. Res. Letters*, **60**, 37–57.

Julian B.R., Miller A. and Foulger G.R., 1998. Non-double-couple earthquakes, 1. Theory. *Rev. Geophys.*, **36**.

Julian B.R., Miller A.D. and Foulger G.R., 1997. Non-double-couple earthquake mechanisms at the Hengill-Grensdalur volcanic complex, southwest Iceland. *Geophys. Res. Lett.*, **24**, 743–746.

Kawasaki I. and Tanimoto T., 1981. Radiation patterns of body waves due to the seismic dislocation occuring in an anisotropic source medium. *Bull. Seismol. Soc. Am.*, **71**, 37–50.

Pšenčík I. and Teles T., 1996. Point source radiation in inhomogeneous anisotropic structures. *PAGEOPH*, **148**, 591–623.

Rümpker G. and Kendall J., 2002. A Maslov-propagator seismogram for weakly anisotropic media. *Geophys. J. Int.*, **150**, 23–36.

Scholz C.H., 1997. *The Mechanics Of Earthquakes And Faulting.* Cambridge University Press.

Šílený J. and Vavryčuk V., 2002. Can unbiased source be retrieved from anisotropic waveforms by using an isotropic model of the medium. *Tectonophysics*, **356**, 125–138.

Silver G. and Jordan T., 1982. Optimal estimation of the scalar seismic moment. *Geophys. J. R. astr. Soc.*, **70**, 755–787.

Solomon S.C. and Julian B.R., 1974. Seismic constraints on ocean-ridge mantle structure: anomalous fault plane solutions from first motions. *Geophys. J. R. astr. Soc.*, **38**, 265–285.

Sykes L.R., 1972. Mechanism of earthquakes and nature of faulting on the mid-ocean ridges. *J. Geophys. Res.*, **72**, 5–27.

Vavryčuk V., 1993. Crustal anisotropy from local observations of shear-wave splitting in West Bohemia, Czech Republic. *Bull. Seismol. Soc. Am.*, **83**, 1420–1441.

Vavryčuk V., 2002. Non-double-couple earthquakes of 1997 January in West Bohemia, Czech Republic: evidence of tensile faulting. *Geophys. J. Int.*, **149**, 364–373.